



## Non-Dyadic Wavelets Based Computational Technique for the investigation of Bagley-Torvik Equations

Harpreet Kaur<sup>1</sup>, Ratesh Kumar<sup>2</sup> and Geeta Arora<sup>2</sup>

<sup>1</sup>Department of Mathematics, I.K. Gujral Punjab Technical University, Kapurthala, India

<sup>2</sup>Department of Mathematics, Lovely Professional University, Phagwara, India.

(Corresponding author: Ratesh Kumar)

(Received 02 May 2019, Revised 10 July 2019, Accepted 08 August 2019)

(Published by Research Trend, Website: www.researchtrend.net)

**ABSTRACT:** The aim of the proposed study is to develop a new hybrid method using the non-dyadic wavelets for the investigation of Bagley-Torvik Equation. Non-dyadic wavelets are used to estimate the solution by series approximation. To handle the fractional derivatives and integrals in the problem, Caputo sense definition of derivatives and Riemann-Liouville definitions of integrals are used. Numerical solution has been produced for five different fractional Bagley-Torvik Equations to establish the competency of the proposed method.

**Keywords:** Non-dyadic wavelets, Bagley-Torvik Equation, Caputo derivatives, Quasi-linearization, Fractional differential equations (65L10)

### I. INTRODUCTION

Fractional calculus is a branch of applied mathematics which emerges as a great tool in explaining the physical and chemical phenomenon with alienate kinetics having microscopic complex behavior. There are fractional differential models which have a non-differentiable but continuous solution such as Weierstrass type functions [1]. These kinds of characteristics are not possible to explain with the help of ordinary or partial differential models. Earlier the field of fractional calculus was purely mathematical without any visible application but in these days, fractional calculus has gained a huge importance in the field of science and technology because of its application in the various field like theory of thermo-elasticity [2], viscoelastic fluids [3], dynamics of earthquakes [4], fluid dynamics [5], etc . Bagley-Torvik equation is one of the most important fractional models in the field of viscoelastic fluids. In this model, Bagley and Torvik have studied the motion of rigid plate immersed into the Newtonian fluid. It is found in the experiment that retarding force is proportional to the fractional derivative of the displacement instead of the velocity. It has been observed during the experiment that fractional model is superior to the integer-order model for the prediction of characteristics of the same material. But general closed-form solution for fractional Bagley-Torvik equation has yet not been established. Therefore, many researchers are involved in developing the various numerical and semi-analytic schemes for investigating the different phenomena governed by the Bagley-Torvik equation such as Adomian decomposition method [6], Variational iteration method (VIM) [7], Homotopy analysis method[8], Generalized Taylor collocation method [9], Haar Wavelet Method (HWM) dilation factor 2 [10], Fractional iteration method [11], Bessel collocation method [12], Chebyshev wavelet method [13], Fractional Taylor series Method [14], Hybrid functions approximation [15], Gegenbauer Wavelet

Method [16], Reproducing kernel algorithm [17], Sumudu transformation method [18] etc.

But the study of characteristics of different materials governed by Bagley Torvik equations has yet not been investigated by non-dyadic wavelet-based technique. Wavelets are one of the modernistic orthonormal functions which have a capability of dilation and translation. Because of these properties, numerical techniques which involve wavelets bases are showing the qualitative improvement in contrast with other methods. In literature, dyadic wavelets are in preponderance. In 1995, Chui and Lian [19] has developed the non-dyadic wavelets by using the process of multiresolution analysis. In 2018, Mittal and Pandit have used the non-dyadic wavelets [20-22] for solving the various types of differential equations and found that these wavelet bases are equally competent in solving the various types of mathematical models governed by differential equations. Also, it was shown by them that the non-dyadic wavelet has a faster rate of convergence as compared to the dyadic wavelets. Moreover, investigation of characteristics of the solution to the Bagley Torvik equation has yet not been done by non-dyadic wavelet methods. This encourages us to develop a new technique using non-dyadic wavelet for analyzing the behavior of systems governed by the Bagley Torvik equation.

The prime purpose of proposed work is to establish a new computational technique for obtaining the solution of following types of Bagley Torvik equations emerging in the field of fluid dynamics using non-dyadic wavelet bases.

$$\left\{ \begin{array}{l} \alpha D^2 x(t) + \beta D^{\frac{3}{2}} x(t) + \gamma D^{\frac{1}{2}} x(t) + x(t) = g(t) \\ \text{with} \\ \text{boundary conditions} \\ x(0) = \delta_0, x(1) = \delta_1 \\ \text{or} \\ x(0) = \delta_2, x'(1) = \delta_3 \end{array} \right. \quad (1)$$

The manuscript follows the sequence of sections as described: In section II, the basic definitions of fractional calculus are given. In section III, explicit forms of non-dyadic parent wavelets with their families and procedure to find their integrals have been explained briefly. Representation of the solution using non-dyadic wavelets is explained in section IV. Section V explains the method of solution using non-dyadic wavelets. In section VI, argument for the convergence of the technique is given. In section VII, solutions of five different examples of Bagley Torvik equations are produced using the present method to analyze the efficiency and performance of the present method. In section VII, the conclusion drawn from the results and in future research idea is given.

## II. SOME BASIC DEFINITIONS OF FRACTIONAL CALCULUS

### A. Mittag-Leffler function

It is an extension of exponential function which has a huge importance in the field of fractional calculus. It has two forms of expression as given below

- i. One Parameter Mittag-Leffler Function [23] for a set of complex numbers and any positive real no  $\alpha$  is defined as

$$E_{\alpha} = \sum_{m=0}^{\infty} \frac{z^m}{\Gamma(\alpha m + 1)}, \alpha > 0, \alpha \in \mathbb{R}, z \in \mathbb{C} \quad (2)$$

- ii. Two-Parameter Mittag-Leffler Function [23] for a set of complex numbers and for positive real no's  $\alpha, \beta$  is defined as

$$E_{\alpha, \beta} = \sum_{m=0}^{\infty} \frac{z^m}{\Gamma(\alpha m + \beta)}, \alpha, \beta > 0, \alpha, \beta \in \mathbb{R}, z \in \mathbb{C} \quad (3)$$

### B. Riemann-Liouville fractional integral operator [23]

The fractional integral operator defined by the mathematician Riemann-Liouville for the positive real nos.  $\alpha, a, t$  over the interval  $[a, b]$  is given by

$${}_R I_a^{\alpha} f(t) = \frac{1}{\Gamma(\alpha)} \int_a^t f(z) (t-z)^{\alpha-1} dz \quad (4)$$

where  $\alpha$  denotes the order of derivative and  $t \in [a, b]$ .

### C. Riemann-Liouville fractional differential operator [23]

The fractional differential operator defined by the mathematician Riemann-Liouville for the positive real nos.  $\alpha, a, t$  over the interval  $[a, b]$  is given by

$${}_R L D_a^{\alpha} f(t) = \begin{cases} \frac{1}{\Gamma(m-\alpha)} \frac{d^m}{dt^m} \int_a^t \frac{f(z)}{(t-z)^{\alpha-m+1}} dz, & m-1 < \alpha < m \in \mathbb{N} \\ \frac{d^m}{dt^m} f(t), & \alpha = m \in \mathbb{N} \end{cases} \quad (5)$$

where  $\alpha$  denotes the order of derivative and  $t \in [a, b]$ .

### D. Caputo fractional differential operator [23]

The fractional differential operator defined by the Italian mathematician Caputo for the positive real nos.  $\alpha, a, t$  is

$${}_C D_a^{\alpha} f(t) = \begin{cases} \frac{1}{\Gamma(m-\alpha)} \int_a^t \frac{f^m(z)}{(t-z)^{\alpha-m+1}} dz, & m-1 < \alpha < m \in \mathbb{N} \\ \frac{d^m}{dt^m} f(t), & \alpha = m \in \mathbb{N} \end{cases} \quad (6)$$

where  $\alpha$  denotes the order of derivative and  $t \in [a, b]$ .

## III. INTEGRALS OF NON-DYADIC HAAR WAVELET

The explicit expressions for Haar function the father wavelet, symmetric and antisymmetric mother wavelets for non-dyadic wavelet family with dilation factor three [19, 22] are given below

$$\text{Haar scaling function } \varphi(t) = \begin{cases} 1 & 0 \leq t < 1 \\ 0 & \text{elsewhere} \end{cases} \quad (7)$$

Haar symmetric wavelet function

$$\psi_1(t) = \frac{1}{\sqrt{2}} \begin{cases} -1 & 0 \leq t < \frac{1}{3} \\ 2 & \frac{1}{3} \leq t < \frac{2}{3} \\ -1 & \frac{2}{3} \leq t < 1 \\ 0 & \text{elsewhere} \end{cases} \quad (8)$$

Haar antisymmetric wavelet function

$$\psi_2(t) = \sqrt{\frac{3}{2}} \begin{cases} 1 & 0 \leq t < \frac{1}{3} \\ 0 & \frac{1}{3} \leq t < \frac{2}{3} \\ -1 & \frac{2}{3} \leq t < 1 \\ 0 & \text{elsewhere} \end{cases} \quad (9)$$

The main difference which makes the non-dyadic wavelets better than the dyadic wavelets is that only one mother wavelet is responsible for the construction of whole wavelet family but in case of non-dyadic wavelets, two mother wavelets with different shapes are responsible for the construction of the whole family. Because of this fact, non-dyadic wavelets increase the convergence rate of the solution. Wavelets represented by Eqn. (8, 9) are the mother wavelets which generate the whole non-dyadic wavelet family. A multi-resolution analysis is used to get the whole non-dyadic Haar wavelet family as described below.

### A. Multi-resolution analysis

Multi-resolution analysis for space  $L_2(\mathbb{R})$  is defined as a sequence of closed subspace  $W_j, V_j \subset L_2(\mathbb{R}), j \in \mathbb{Z}$  which has the properties as given below

- a)  $\phi(t) \in V_0 \Rightarrow \phi(3^j t) \in V_j$
- b)  $\phi(t) \in V_0 \Rightarrow \phi(3^j t - k) \in V_j$
- c)  $\psi^i(t) \in W_0^i, i = 1, 2 \Rightarrow \psi^i(3^j t) \in W_j^i$
- d)  $\psi^i(t) \in W_0^i, i = 1, 2 \Rightarrow \psi^i(3^j t - k) \in W_j^i$
- e)  $W_j = W_j^1 \oplus W_j^2 = \bigoplus W_j^i, i = 1, 2$
- f)  $\dots \subset V_0 \subset V_1 \subset V_2 \subset V_3 \subset V_4 \subset \dots$
- g)  $\dots \perp W_0 \perp W_1 \perp W_2 \perp W_3 \perp W_4 \perp \dots$
- h)  $V_j = V_0 + \sum_{i=0}^{j-1} W_j^1 + \sum_{i=0}^{j-1} W_j^2$

i)  $\phi(t) \in V_0$  implies  $\phi(t-k) \in V_0; k \in \mathbb{Z}$  and it forms Riesz basis in  $V_0$

Now by applying MRA, generalized form of non-dyadic Haar wavelet family is obtained as follows:

$$h_i(t) = \varphi(t) = \begin{cases} 1 & 0 \leq t < 1 \\ 0 & \text{elsewhere} \end{cases} \text{ for } i = 1$$

$$h_i(t) = \psi^1(3^j t - k) = \frac{1}{\sqrt{2}} \begin{cases} -1 & \alpha_1(i) \leq t < \alpha_2(i) \\ 2 & \alpha_2(i) \leq t < \alpha_3(i) \\ -1 & \alpha_3(i) \leq t < \alpha_4(i) \\ 0 & \text{elsewhere} \end{cases} \text{ for } i = 2, 4, \dots, 3p-1 \quad (10)$$

$$h_i(t) = \psi^2(3^j t - k) = \frac{1}{\sqrt{2}} \begin{cases} 1 & \alpha_1(i) \leq t < \alpha_2(i) \\ 0 & \alpha_2(i) \leq t < \alpha_3(i) \\ -1 & \alpha_3(i) \leq t < \alpha_4(i) \\ 0 & \text{elsewhere} \end{cases} \text{ for } i = 3, 6, \dots, 3p \quad (11)$$

where  $\alpha_1(i) = \frac{k}{p}, \alpha_2(i) = \frac{3k+1}{3p}, \alpha_3(i) = \frac{(3k+2)}{3p}, \alpha_4(i) = \frac{k+1}{p}, p = 3^j, j = 0, 1, 2, \dots, k = 0, 1, 2, \dots, p-1$ .

Here  $i, j, k$  respectively represent the wavelet number, level of resolution (dilation) and translation parameters of wavelets family. The values of  $i$  (for  $i > 1$ ) can be calculated with the help of  $j, k$  by using the following relations  $\begin{cases} i-1 = 3^j + 2k & \text{for even } i \\ i-2 = 3^j + 2k & \text{for odd } i \end{cases}$ . By using this relation for different dilation and translations of  $h_2(t), h_3(t)$ , we will get the wavelet family as  $h_1(t), h_2(t), h_3(t), h_4(t), h_5(t), h_6(t), \dots$  where  $h_2(t)$  and  $h_3(t)$  are also called mother wavelets and rest all the wavelets which we have obtained from mother wavelet are called daughter wavelets.

Now one can easily integrate Eqn. (7, 11) desired number of times over the interval  $[A, B)$  by using Riemann Liouville Integral formula as given below

$$q_{\alpha,i}(t) = \frac{1}{\Gamma(\alpha)} \int_A^t h_i(x) (t-x)^{\alpha-1} dx ;$$

$$0 \leq \alpha \leq m, m = 1, 2, 3, \dots, i = 1, 2, 3, \dots, 3p \quad (12)$$

After evaluating the above integrals, we get  $q_{\beta,i}(t)$ 's for  $i = 2, 4, 6, 8, \dots, 3p-1$  are given below  
 {for  $0 \leq t \leq \alpha_1(i)$   $q_{\beta,i}(t) = 0$

for  $\alpha_1(i) \leq t \leq \alpha_2(i)$

$$q_{\beta,i}(t) = \frac{1}{\sqrt{2}} \frac{-1}{\Gamma(\beta+1)} (t - \alpha_1(i))^\beta$$

for  $\alpha_2(i) \leq t \leq \alpha_3(i)$

$$q_{\beta,i}(t) = \frac{1}{\sqrt{2}} \frac{1}{\Gamma(\beta+1)} [-(t - \alpha_1(i))^\beta + 3(t - \alpha_2(i))^\beta]$$

for  $\alpha_3(i) \leq t \leq \alpha_4(i)$

$$q_{\beta,i}(t) = \frac{1}{\sqrt{2}} \frac{1}{\Gamma(\beta+1)} [-(t - \alpha_1(i))^\beta + 3(t - \alpha_2(i))^\beta - 3(t - \alpha_3(i))^\beta]$$

for  $\alpha_4(i) \leq t \leq 1$

$$q_{\beta,i}(t) = \frac{1}{\sqrt{2}} \frac{1}{\Gamma(\beta+1)} [-(t - \alpha_1(i))^\beta + 3(t - \alpha_2(i))^\beta - 3(t - \alpha_3(i))^\beta + (t - \alpha_4(i))^\beta] \quad (13)$$

$q_{\beta,i}(t)$ 's for  $i = 3, 5, 7, 9, \dots, 3p$  are given by  
 {for  $0 \leq t \leq \alpha_1(i)$   $q_{\beta,i}(t) = 0$

for  $\alpha_1(i) \leq t \leq \alpha_2(i)$

$$q_{\beta,i}(t) = \sqrt{\frac{3}{2}} \frac{1}{\Gamma(\beta+1)} (t - \alpha_1(i))^\beta$$

for  $\alpha_2(i) \leq t \leq \alpha_3(i)$

$$q_{\beta,i}(t) = \sqrt{\frac{3}{2}} \frac{1}{\Gamma(\beta+1)} [(t - \alpha_1(i))^\beta - (t - \alpha_2(i))^\beta]$$

for  $\alpha_3(i) \leq t \leq \alpha_4(i)$

$$q_{\beta,i}(t) = \sqrt{\frac{3}{2}} \frac{1}{\Gamma(\beta+1)} [(t - \alpha_1(i))^\beta - (t - \alpha_2(i))^\beta - (t - \alpha_3(i))^\beta]$$

for  $\alpha_4(i) \leq t \leq 1$

$$q_{\beta,i}(t) = \sqrt{\frac{3}{2}} \frac{1}{\Gamma(\beta+1)} [(t - \alpha_1(i))^\beta - (t - \alpha_2(i))^\beta - (t - \alpha_3(i))^\beta + (t - \alpha_4(i))^\beta] \quad (14)$$

$$q_{\beta,i}(t) = \frac{t^\beta}{\Gamma(\beta+1)} \text{ for } i = 1 \quad (15)$$

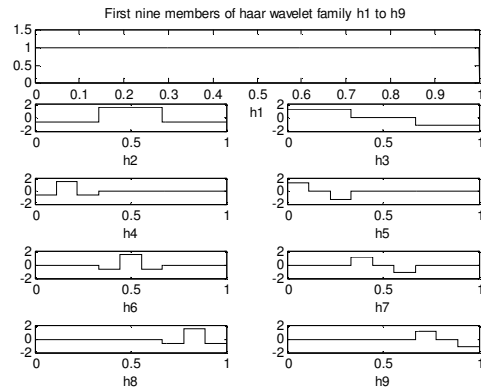


Fig. 1. Non-dyadic Haar wavelets.

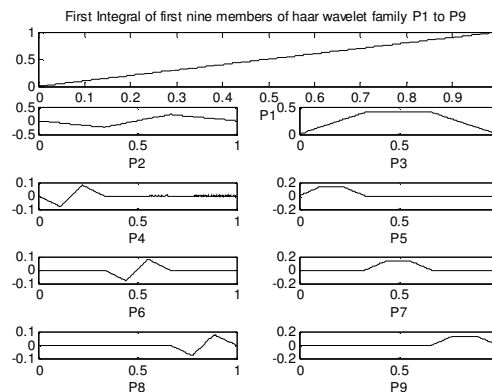


Fig. 2. First integral of wavelets.

#### IV. APPROXIMATION OF SOLUTION

Using properties of non-dyadic wavelets as explained in section III, any function  $x(t) \in L_2(R)$  can be expressed as

$$x(t) = \sum_{i=0}^{\infty} a_i h_i(t) = a_1 h_1(t) + \sum_{\text{even } i} a_i \psi^1(3^j t - k) + \sum_{\text{odd } i > 1} a_i \psi^2(3^j t - k) \quad (16)$$

Here  $a_i$ 's are the wavelet coefficients whose values are to be determined by the proposed method. But for the computational purpose, one can consider a finite number of terms. By considering the first  $3p$  terms to approximate the function  $u(t)$  we get

$$x(t) \approx u_{3p} = \sum_{i=0}^{3p} a_i h_i(t)$$

where  $p = 3^j, j = 0, 1, 2, \dots$  (17)

#### V. METHOD OF SOLUTION BASED ON NON-DYADIC HAAR WAVELETS

Consider the Bagley Torvik equation

$$\alpha D^2 x(t) + \beta D^{\frac{3}{2}} x(t) + \gamma D^{\frac{1}{2}} x(t) + \delta x(t) = g(t) \quad (18)$$

with initial conditions  $x(0) = \delta_2, x'(0) = \delta_3$ , and  $\alpha, \beta, \gamma, \delta$  are the arbitrary constants.

Now the solution  $x(t)$  for the above equation can be obtained using the following steps

**Step 1:** Approximate the highest order derivative present in the equation (18) (i.e.  $D^2 x(t)$ ) using the non-dyadic wavelet bases as

$$D^2 x(t) = \sum_{i=0}^{3p} a_i h_i(t) = a_1 h_1(t) + \sum_{\text{even } i} a_i \psi^1(3^j t - k) + \sum_{\text{odd } i > 1} a_i \psi^2(3^j t - k) \quad (19)$$

where  $a_i$ 's for  $i = 0, 1, 2, \dots, 3p$  are the nondyadic wavelet coefficients

**Step 2:** By integrating the equation (19) within the limits 0 to  $t$ , we get

$$x'(t) = \sum_{i=0}^{3p} a_i q_{1,i}(t) + y'(0) = \sum_{i=0}^{3p} a_i q_{1,i}(t) + \delta_3 \quad (20)$$

Again, integrating the equation (20) within the limits 0 to  $t$ , we get

$$x(t) = \sum_{i=0}^{3p} a_i q_{2,i}(t) + \delta_3 t + y(0) = \sum_{i=0}^{3p} a_i q_{2,i}(t) + \delta_3 t + \delta_2 \quad (21)$$

**Step 3:** Differentiate the Eqn. (21) using Caputo definition of fractional derivatives we get

$$\begin{aligned} D^{\frac{1}{2}} x(t) &= \sum_{i=0}^{3p} a_i q_{\frac{3}{2},i}(t) + 2 \delta_3 \sqrt{\frac{t}{\pi}} \\ D^{\frac{3}{2}} x(t) &= \sum_{i=0}^{3p} a_i q_{\frac{1}{2},i}(t) + \delta_3 \frac{1}{\sqrt{\pi t}} \end{aligned} \quad (22)$$

**Step 4:** Using Eqns. (19-22), Eqn. (18) becomes

$$\begin{aligned} \alpha \sum_{i=0}^{3p} a_i h_i(t) + \beta \left[ \sum_{i=0}^{3p} a_i q_{\frac{1}{2},i}(t) + \delta_3 \frac{1}{\sqrt{\pi t}} \right] + \\ \gamma \left[ \sum_{i=0}^{3p} a_i q_{\frac{3}{2},i}(t) + 2 \delta_3 \sqrt{\frac{t}{\pi}} \right] + \delta \left[ \sum_{i=0}^{3p} a_i q_{2,i}(t) + \delta_3 t + \delta_2 \right] = g(t) \end{aligned}$$

After simplification, we get

$$\sum_{i=0}^{3p} a_i [\alpha h_i(t) + \beta q_{\frac{1}{2},i}(t) + \gamma q_{\frac{3}{2},i}(t) + \delta q_{2,i}(t)] = g(t) - \left[ \beta \delta_3 \frac{1}{\sqrt{\pi t}} + 2\gamma \delta_3 \sqrt{\frac{t}{\pi}} + \delta(\delta_3 t + \delta_2) \right] \quad (23)$$

**Step 4:** After Discretizing the Eqn. (23) using the collocation points we get the following matrix system

$$aH = F \quad (24)$$

Then using the Thomas algorithm, we obtained the wavelet coefficients  $a_i$ 's. Then by substituting the values of wavelet coefficients  $a_i$ 's in Eqn. (21), We get the non-dyadic wavelet-based solution of Bagley Torvik equations with the given initial conditions. Similarly, by using the above steps we find the solution of Bagley Torvik equations with the given boundary conditions.

#### VI. CONVERGENCE ANALYSIS

It has been proved by Mittal and Pandit [24] that if  $x(t) \in L^2(R)$  such that  $|x^m(t)| \leq M, \forall t \in (0,1)$  where  $M$  is any real constant and  $x(t)$  is approximated by Non-dyadic (Scale 3) Haar wavelet family as given below:

$$x_{3p}(t) = \sum_{i=0}^{3p} a_i h_i(t) \quad (25)$$

Then the error bound for the solution  $x(t)$  using  $L_2$ -norm is calculated as

$$\|x(t) - x_{3p}(t)\| \leq \left(\frac{2}{3}\right)^{2(m-\alpha)} \frac{8M^2}{(\Gamma(m-\alpha+1))^2} \left(\frac{3^{-2(j+1)(m-\alpha+1)}}{1-3^{-2(m-\alpha)+1}}\right) \quad (26)$$

Clearly, the error bound is inversely proportional to the level of resolution which ensures the convergence of the approximated solution to exact solution with the increase in the level of resolution  $j$ . Moreover, if we know the exact values of  $m, \alpha$  and  $M$ , then the maximum value of error bound can also be calculated.

#### VII. ERROR ANALYSIS BY NUMERICAL EXPERIMENTS

To describe the appropriateness of the proposed technique for the Bagley Torvik equation of fractional order, solutions of five different problems obtained by the proposed computational technique have been analyzed and absolute errors are calculated to check the efficiency of the present scheme with the help of following formulas

$$\text{Absolute error} = |x_{\text{exact}}(t_i) - x_{\text{num}}(t_i)| \quad (27)$$

where  $t_i$  represents the collocation points of the domain.

**Numerical Experiment No. 1:**  $D^2 x + D^{\frac{3}{2}} x + x = t^2 + 4\sqrt{\frac{t}{\pi}} + 2$  under the following boundary constraints  $x(0) = 0, x(1) = 1$  (28)

Exact solution of the problem is  $x(t) = t^2$

After applying the method of solution discussed in section 5 the following solution is proposed

$$x(t) = \sum_{i=1}^{3p} a_i [q_{2,i}(t) - t q_{2,i}(1)] + t \quad (29)$$

$a_i$ 's are the wavelets coefficients which will be obtained by the following procedure and  $q_{j,i}$ 's are the wavelets integrals which have been already calculated in section 3.

After applying the proposed scheme on the experiment 1. Eqn. (28) is reduced to the following system

$$\sum_{i=0}^{3p} a_i \left[ \sqrt{\pi t} \left( h_i(t) + q_{2,i}(t) + q_{2,i}(t) \right) - \left( \sqrt{\pi t^3} + 1 \right) q_{2,i}(1) \right] = 4t + 1 + \sqrt{\pi} \left[ t^{\frac{5}{2}} - t^{\frac{3}{2}} + 2t^{\frac{1}{2}} \right] \quad (30)$$

After Discretizing the Eqn. (30) using the collocation points we get the following matrix system

$$aH = F \quad (31)$$

**Table 1: Comparison of results achieved with other methods in the existing literature for Experiment No.1**

t	Exact Solution	Approximated Solution	Present Method(E*)	RKA(E*)[17]	VIM(E*)[7]	HAM(E*)[8]
0.1	0.01	0.0100000000000000 006938893903907	6.93889390390723e-18	0	0.5487432e-4	2.3265e-13
0.2	0.04	0.0400000000000000 0000000000000000	0	0	0.6312556e-3	1.4385e-11
0.3	0.09	0.0900000000000000 0000000000000000	0	0	0.2665571e-2	6.1890e-11
0.4	0.16	0.1600000000000000 027755575615628	2.77555756156289e-17	0	0.7480121e-2	2.2736e-11
0.5	0.25	0.2500000000000000 0000000000000000	0	2.77555756156289e-17	0.1679592e-1	1.3680e-10
0.6	0.36	0.3600000000000000 0000000000000000	0	5.55111512312578e-17	0.3277307e-1	3.5678e-11
0.7	0.49	0.4900000000000000 055511151231257	5.55111512312578e-17	5.55111512312578e-17	0.5806535e-1	2.6188e-10
0.8	0.64	0.6400000000000000 0000000000000000	0	1.11022302545678e-17	0.9588508e-1	4.3416e-10
0.9	0.81	0.8100000000000000 0000000000000000	0	1.11022302545678e-17	0.1500768448	1.0816e-10

E\* (Absolute Error)

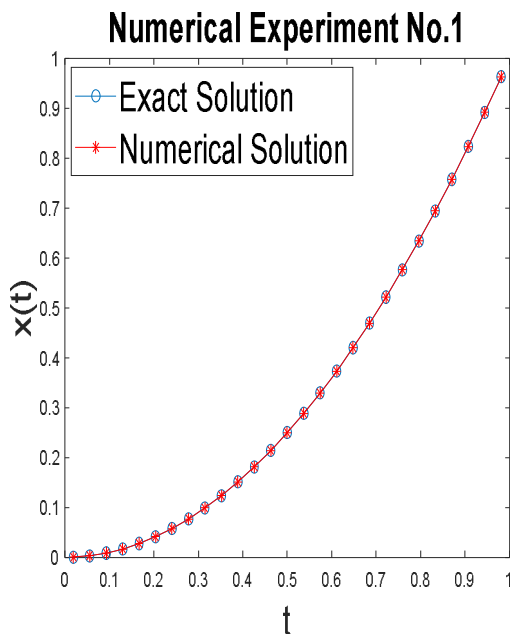


**Fig. 1.** Comparison of exact and numerical solution of Numerical experiment No.1 at the level of resolution J=2.

After solving the above matrix system, we get the values of  $a_i$ 's which will be used to find out the solution. Results achieved by the proposed technique are conferred by the graphs and tables for the better visibility of accuracy.

Fig. 3 and Table 1 demonstrate the clearly visible agreement in the exact and approximated solutions. In Table 1, results achieved by the present technique are compared with other method existing in the recent literature and found it outperform over others methods like Variational Iteration Method (VIM) [7], Homotopy asymptotic method (HAM) [8], Reproducing Kernel Analysis (RKA) [17], which demonstrates the superiority and reliability of the method.

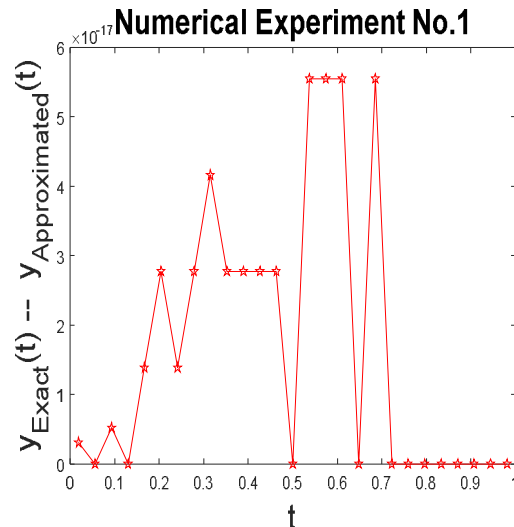


**Fig. 2.** Absolute error at the different collocation points considered for the solution of Numerical experiment No.1.

**Numerical Experiment No. 2:**

$$D^2x(t) + 0.5 D^{\frac{1}{2}}x(t) + x(t) = 3 + t^2 \left( \frac{1}{\Gamma(2.5)} t^{-0.5} + 1 \right) \text{ w.r.t}$$

B. C's  $x(0) = 0, x(1) = 2$  (32)

Exact solution of the problem is  $x(t) = t^2 + 1$ .  
 After applying the method of solution discussed in section 5 the following solution is proposed

$$x(t) = \sum_{i=1}^{3p} a_i [q_{2,i}(t) - tq_{2,i}(1)] + t + 1 \quad (33)$$

$a_i$ 's are the wavelets coefficients which will be obtained by the following procedure and  $q_{j,i}$ 's are the wavelets integrals which have been already calculated in section

3. After applying the proposed technique on the experiment no. 2. Eqn. (32) is reduced to the following system

$$\sum_{i=0}^{3p} a_i \left[ \left( h_i(t) + \frac{1}{2} q_{\frac{3}{2},i}(t) + q_{2,i}(t) \right) - \left( \frac{t^{\frac{1}{2}}}{\sqrt{\pi}} + t \right) q_{2,i}(1) \right] = t^2 - t + 2 + \left[ \frac{4}{3\sqrt{\pi}} t^{\frac{3}{2}} - \frac{1}{\sqrt{\pi}} t^{\frac{1}{2}} \right] \quad (34)$$

After Discretizing the Eqn. (34) using the collocation points we get the following matrix system  
 $aH = F$

**Table 2: Comparison of results achieved with other methods in the existing literature for Experiment No. 2.**

t	Exact Solution	Approximated Solution	Present Method(E*)	RKA(E*) [17]
0.1	1.01	1.01000000000000000000	0	1.932676241e-12
0.2	1.04	1.04000000000000000000	0	3.161981788e-11
0.3	1.09	1.09000000000000000000	0	3.679907490e-10
0.4	1.16	1.16000000000000000000	0	3.661697390e-09
0.5	1.25	1.25000000000000000000	0	3.300057339e-09
0.6	1.36	1.36000000000000000000	0	2.745960126e-09
0.7	1.49	1.49000000000000022204	2.22044604925031e-16	2.096272045e-10
0.8	1.64	1.64000000000000000000	0	1.404942829e-11
0.9	1.81	1.81000000000000000000	0	7.004619107e-12

E\* (Absolute Error)

After solving the above matrix system, we get the vales of  $a_i$ 's which will be used to find out the solution. It can be observed from the Table 2 and Fig. 5, that the results achieved by the proposed method agree well with exact solution, which demonstrate the high efficiency of the proposed technique to solve these kinds of problems.

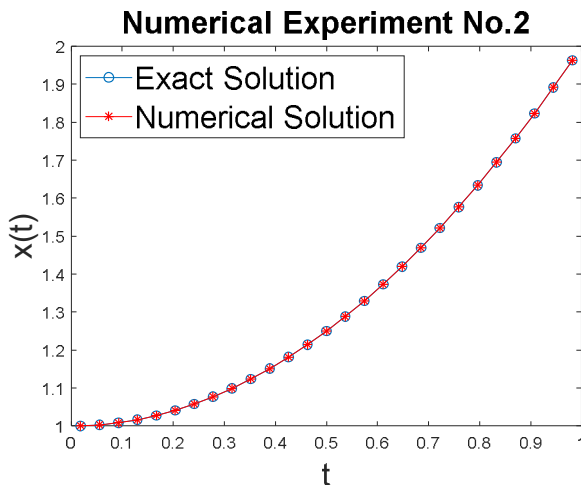


**Fig. 5.** Comparison of exact and numerical solution of numerical experiment No. 2 at the level of resolution J=2.

From Table 2, one can say that the proposed technique is a strong solver in terms of better accuracy as compare to other method [17] given in the Table 2. Fig. 6 is showing the errors at the different collocation points.

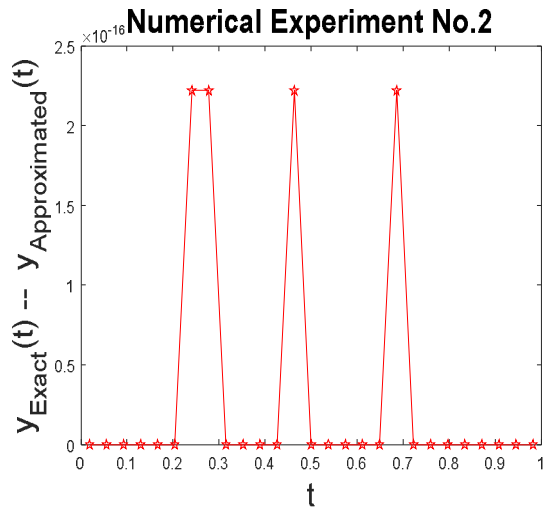


**Fig. 3.** Absolute error at the different collocation points considered for the solution of Numerical experiment No.2.

**Numerical Experiment No. 3:**  $D^2x(t) + D^{\frac{1}{2}}x(t) + x(t) = 2 + t^2 \left(\frac{2}{\Gamma(2.5)}t^{-0.5} + 1\right) - t \left(\frac{1}{\Gamma(1.5)}t^{-0.5} + 1\right)$  subjected to the boundary condition  $x(0) = 0, x(1) = 0$  (35)

Exact solution of the problem is  $x(t) = t^2 - t$   
 After applying the method of solution discussed in the section 5 the following solution is obtained by the proposed method

$$x(t) = \sum_{i=1}^{3p} a_i [q_{2,i}(t) - tq_{2,i}(1)] \quad (36)$$

$a_i$ 's are the wavelets coefficients which will be obtained by the procedure discussed above and  $q_{j,i}$ 's are the wavelets integrals which has been already calculated in section 3.

Table 3 depicting the performance of the method in contrast with other method existing in the recent literature. It validates the high efficiency and performance of the method. Getting high accuracy for a small number of grid points makes it strong solver for these kinds of mathematical models. Fig. 7 demonstrates that the results achieved with the proposed technique agree well with exact solution and Fig. 8 explains the errors in the solution at the different collocation points.

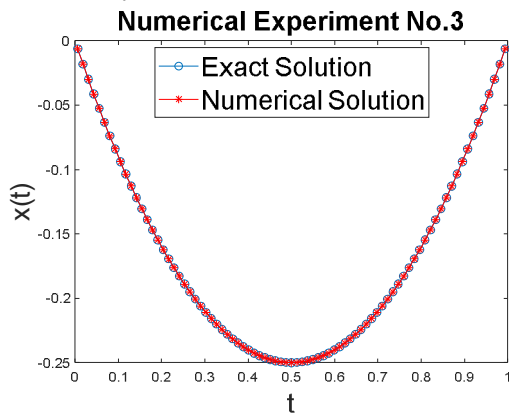


**Fig. 4.** Comparison of exact and numerical solution of Numerical experiment No. 3 at the level of resolution  $J=2$ .

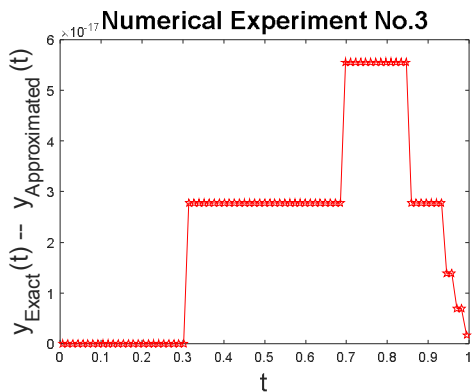


**Fig. 5.** Absolute error at the different collocation points considered for the solution of Numerical experiment No. 3.

**Numerical Experiment No. 4:**

$D^2x(t) + D^{\frac{3}{2}}x(t) + x(t) = t + \frac{1}{\sqrt{\pi t}} + 1$  subjected to the boundary condition  $x(0) = 0, x'(1) = 1$  (37)

Analytic solution of the problem is  $x(t) = t + 1$   
 By using the method of solution discussed in the section 3, we proposed the following solution for the above equations

$$x(t) = \sum_{i=1}^{3p} a_i q_{2,i}(t) + t + 1 \quad (38)$$

$a_i$ 's are the wavelets coefficients which will be obtained by the procedure discussed above and  $q_{j,i}$ 's are the wavelets integrals which has been already calculated in section 3. It is shown in Table 4 and Fig. 10 that results achieved with the proposed technique exactly matching with exact solution with no error. It is also shown in the Table 4 that the results achieved with the proposed technique are superior than the results obtained by the other methods available in the existing literature explains the high level of agreement between the exact and approximated solution.

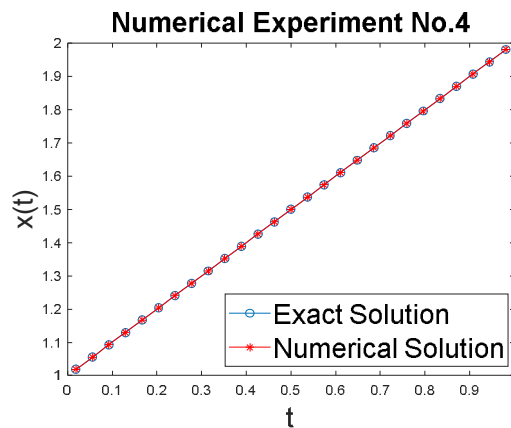


**Fig. 6.** Comparison of exact and numerical solution of Numerical experiment No. 4 at the level of resolution  $J=2$ .

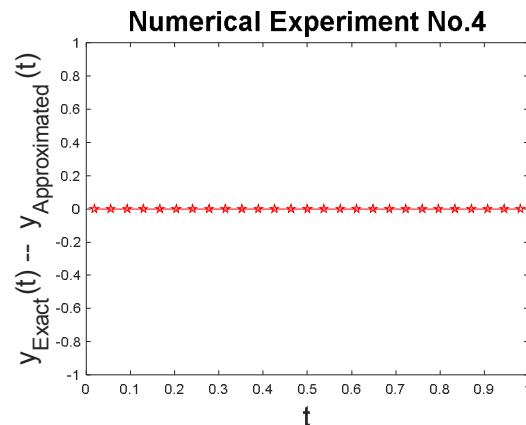


**Fig. 7.** Absolute error at the different collocation points considered for the solution of Numerical experiment No. 4.

**Numerical Experiment No. 5:**

$$D_z^3 x(t) + x(t) = t^5 - t^4 + \frac{128}{7\sqrt{\pi}} t^{\frac{7}{2}} - \frac{64}{5\sqrt{\pi}} t^{\frac{5}{2}} \text{ subjected to the boundary condition } x(0) = 0, x(1) = 0 \quad (39)$$

Exact solution for the problem is  $x(t) = t^5 - t^4$

Using the method of solution explained in section no. 3, Following solution is proposed for the numerical experiment no. 5

$$x(t) = \sum_{i=1}^{3p} a_i [q_{2,i}(t) - tq_{2,i}(1)] \quad (40)$$

$a_i$ 's are the wavelets coefficients which will be obtained by the procedure discussed above and  $q_{j,i}$ 's are the wavelets integrals which has been already calculated in section 3

**Table 3: Comparision of results achived with other methods in the existing  $t$  literature for Experiment No. 3.**

$t$	Exact Solution	Approximated Solution	Present Method ( $E^+$ )	RKA( $E^+$ ) [17]
0.1	- 0.0900000000000000	- 0.09000000000000000000000000000000	0	4.178019042e-12
0.2	- 0.1600000000000000	- 0.1600000000000000027755575615629	- 2.77555756156289e-17	6.892891813e-11
0.3	- 0.2100000000000000	- 0.2100000000000000055511151231258	5.55111512312578e-17	8.052572498e-10
0.4	- 0.2400000000000000	- 0.2400000000000000055511151231258	5.55111512312578e-17	8.010652391e-09
0.5	- 0.2500000000000000	- 0.2500000000000000055511151231258	5.55111512312578e-17	7.193844853e-09
0.6	- 0.2400000000000000	- 0.2400000000000000055511151231258	5.55111512312578e-17	5.949374826e-09
0.7	- 0.2100000000000000	- 0.2100000000000000055511151231258	5.55111512312578e-17	4.504783491e-10
0.8	- 0.1600000000000000	- 0.1600000000000000027755575615629	2.77555756156289e-17	2.989430925e-11
0.9	- 0.0900000000000000	- 0.0900000000000000027755575615629	2.77555756156289e-17	1.473612898e-12

$E^+$  (Absolute Error)

**Table 4: Comparision of results achived with other methods in the existing literature for Experiment No. 4.**

$t$	Exact Solution	Approximated Solution	Present Method ( $E^+$ )	RKA( $E^+$ ) [17]	BCM( $E^+$ ) [12]
0.1	1.1	1.1	0	0	9.3742e-16
0.2	1.2	1.2	0	0	3.9634e-15
0.3	1.3	1.3	0	0	4.2834e-15

0.4	1.4	1.4	0	0	3.2975e-15
0.5	1.5	1.5	0	0	2.0455e-15
0.6	1.6	1.6	0	2.220446049E-16	1.0277e-15
0.7	1.7	1.7	0	0	3.4773e-16
0.8	1.8	1.8	0	0	6.9289e-17
0.9	1.9	1.9	0	2.220446049E-16	2.3947e-16

E<sup>\*</sup> (Absolute Error)

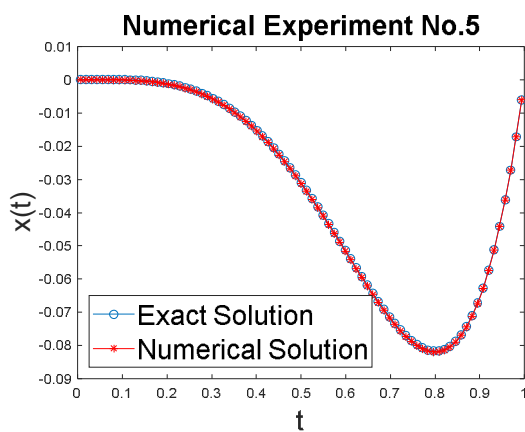


Fig. 8. Comparison of exact and numerical solution of Numerical experiment No. 5 at the level of resolution J=2.

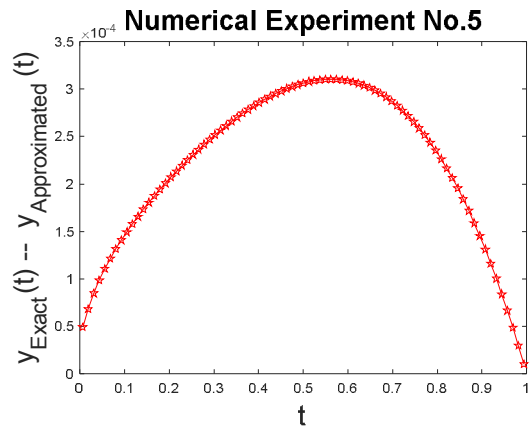


Fig. 9. Absolute error at the different collocation points in Numerical experiment No. 5.

## VIII. CONCLUSION

After looking at the results of five numerical experiments performed with proposed technique, we infer that Bagley-Torvik equation of fractional order can easily be solved by the proposed scheme with less computational cost and high accuracy. For example, in numerical experiment no. 1 level of accuracy obtained is or order  $10^{-17}$  for only 9 collocation points in the first iteration. Moreover, the use of common MATLAB subprograms to solve various types of fractions equations, makes it more

computer friendly. Very good accuracy is obtained for a very small number of collocation points and the results achieved are better than or at par with the other methods existing in the recent literature. It makes the proposed scheme a strong solver for these kinds of fractional differential equations. Therefore, by looking at the performance of the method, we conclude that the given method can be extended to solve other set of fractional differential equations. All the calculations have been performed using the MATLAB 7.

Table 5: Comparison of results achieved by the proposed method with the exact solution for experiment No. 5.

t	Exact Solution	Approximated Solution	Present Method (E <sup>*</sup> )
0.00617284	-1.4429480000E-09	4.9171205846E-05	4.92E-05
0.01851852	-1.1542691000E-07	6.7922819931E-05	6.80E-05
0.0308642	-8.7943672400E-07	8.3907873324E-05	8.48E-05
0.04320988	-3.3354066130E-06	9.5100857199E-05	9.84E-05
0.05555556	-8.9967653980E-06	1.0151360079E-04	1.11E-04
0.06790123	-1.9814020830E-05	1.0157260482E-04	1.21E-04

0.08024691	-3.8140343926E-05	9.3243967138E-05	1.31E-04
0.09259259	-6.6697153309E-05	7.3993891171E-05	1.41E-04
0.10493827	-1.0853969954E-04	4.0900842117E-05	1.49E-04
0.11728395	-1.6702264946E-04	-9.2943502120E-06	1.58E-04
0.12962963	-2.4576567051E-04	-8.0140150666E-05	1.66E-04
0.14197531	-3.4861901510E-04	-1.7543265253E-04	1.73E-04
0.15432099	-4.7962910491E-04	-2.9917635750E-04	1.80E-04
0.16666667	-6.4300411523E-04	-4.5554663647E-04	1.87E-04
0.17901235	-8.4307955932E-04	-6.4885316645E-04	1.94E-04
0.19135802	-1.0842838727E-03	-8.8350400114E-04	2.01E-04
0.2037037	-1.3711039977E-03	-1.1639700577E-03	2.07E-04
0.21604938	-1.7080509673E-03	-1.4947498869E-03	2.13E-04
0.22839506	-2.0996254899E-03	-1.8803346416E-03	2.19E-04
0.24074074	-2.5502835338E-03	-2.3251731862E-03	2.25E-04
0.25308642	-3.0644019109E-03	-2.8336373097E-03	2.31E-04
0.2654321	-3.6462438616E-03	-3.4099870140E-03	2.36E-04
0.27777778	-4.2999246389E-03	-4.0583358614E-03	2.42E-04
0.29012346	-5.0293770928E-03	-4.7826163651E-03	2.47E-04
0.30246914	-5.8383172545E-03	-5.5865454139E-03	2.52E-04
0.31481481	-6.7302099212E-03	-6.4735897242E-03	2.57E-04
0.32716049	-7.7082342397E-03	-7.4469313129E-03	2.61E-04
0.33950617	-8.7752492913E-03	-8.5094329872E-03	2.66E-04
0.35185185	-9.9337596759E-03	-9.6636038485E-03	2.70E-04
0.36419753	-1.1185881097E-02	-1.0911564807E-02	2.74E-04
0.37654321	-1.2533305943E-02	-1.2255014107E-02	2.78E-04
0.38888889	-1.3977268878E-02	-1.3695192856E-02	2.82E-04
0.40123457	-1.5518512420E-02	-1.5232850567E-02	2.86E-04
0.41358025	-1.7157252525E-02	-1.6868210697E-02	2.89E-04
0.42592593	-1.8893144178E-02	-1.8600936200E-02	2.92E-04
0.4382716	-2.0725246971E-02	-2.0430095076E-02	2.95E-04
0.45061728	-2.2651990688E-02	-2.2354125925E-02	2.98E-04
0.46296296	-2.4671140892E-02	-2.4370803509E-02	3.00E-04
0.47530864	-2.6779764510E-02	-2.6477204310E-02	3.03E-04
0.48765432	-2.8974195412E-02	-2.8669672090E-02	3.05E-04
0.5	-3.1250000000E-02	-3.0943783462E-02	3.06E-04
0.51234568	-3.3601942792E-02	-3.3294313448E-02	3.08E-04
0.52469136	-3.6023952003E-02	-3.5715201053E-02	3.09E-04
0.53703704	-3.8509085134E-02	-3.8199514831E-02	3.10E-04
0.54938272	-4.1049494554E-02	-4.0739418453E-02	3.10E-04
0.5617284	-4.3636393083E-02	-4.3326136283E-02	3.10E-04
0.57407407	-4.6260019578E-02	-4.5949918942E-02	3.10E-04
0.58641975	-4.8909604518E-02	-4.8600008887E-02	3.10E-04
0.59876543	-5.1573335587E-02	-5.1264605982E-02	3.09E-04
0.61111111	-5.4238323257E-02	-5.3930833072E-02	3.07E-04
0.62345679	-5.6890566377E-02	-5.6584701554E-02	3.06E-04
0.63580247	-5.9514917752E-02	-5.9211076957E-02	3.04E-04

0.64814815	-6.2095049731E-02	-6.1793644516E-02	3.01E-04
0.66049383	-6.4613419790E-02	-6.4314874745E-02	2.99E-04
0.67283951	-6.7051236116E-02	-6.6755989015E-02	2.95E-04
0.68518519	-6.9388423191E-02	-6.9096925131E-02	2.91E-04
0.69753086	-7.1603587380E-02	-7.1316302911E-02	2.87E-04
0.70987654	-7.3673982508E-02	-7.3391389755E-02	2.83E-04
0.72222222	-7.5575475453E-02	-7.5298066235E-02	2.77E-04
0.7345679	-7.7282511722E-02	-7.7010791659E-02	2.72E-04
0.74691358	-7.8768081044E-02	-7.8502569662E-02	2.66E-04
0.75925926	-8.0003682946E-02	-7.9744913774E-02	2.59E-04
0.77160494	-8.0959292343E-02	-8.0707813004E-02	2.51E-04
0.78395062	-8.1603325119E-02	-8.1359697417E-02	2.44E-04
0.7962963	-8.1902603714E-02	-8.1667403713E-02	2.35E-04
0.80864198	-8.1822322707E-02	-8.1596140806E-02	2.26E-04
0.82098765	-8.1326014400E-02	-8.1109455403E-02	2.17E-04
0.83333333	-8.0375514403E-02	-8.0169197584E-02	2.06E-04
0.84567901	-7.8930927218E-02	-7.8735486380E-02	1.95E-04
0.85802469	-7.6950591824E-02	-7.6766675354E-02	1.84E-04
0.87037037	-7.4391047259E-02	-7.4219318181E-02	1.72E-04
0.88271605	-7.1206998208E-02	-7.1048134226E-02	1.59E-04
0.89506173	-6.7351280585E-02	-6.7205974126E-02	1.45E-04
0.90740741	-6.2774827117E-02	-6.2643785369E-02	1.31E-04
0.91975309	-5.7426632931E-02	-5.7310577875E-02	1.16E-04
0.93209877	-5.1253721134E-02	-5.1153389575E-02	1.00E-04
0.94444444	-4.4201108401E-02	-4.4117251993E-02	8.39E-05
0.95679012	-3.6211770559E-02	-3.6145155825E-02	6.66E-05
0.9691358	-2.7226608169E-02	-2.7178016522E-02	4.86E-05
0.98148148	-1.7184412112E-02	-1.7154639868E-02	2.98E-05
0.99382716	-6.0218291745E-03	-6.0116875623E-03	1.01E-05

E (Absolute Error)

**Conflict of Interest:** Author has no any conflict of interest.

## REFERENCES

- [1]. Zahle, M., & Ziezold, H. (1996). Fractional derivatives of Weierstrass-type functions. *Journal of Computational and Applied Mathematics*, **76**(1996), 265–275.
- [2]. Povstenko, Y. Z. (2009). Thermoelasticity that uses fractional heat conduction equation. *Journal of Mathematical Sciences*, **162**(2), 296–305. <https://doi.org/10.1007/s10958-009-9636-3>
- [3]. Tripathi, D., Pandey, S. K., & Das, S. (2010). Peristaltic flow of viscoelastic fluid with fractional Maxwell model through a channel. *Applied Mathematics and Computation*, **215**(10), 3645–3654. <https://doi.org/10.1016/j.amc.2009.11.002>
- [4]. Lopes, A. M., Tenreiro Machado, J.A., Pinto, C. M. A., & Galhano, A. M. S. F. (2013). Fractional dynamics and MDS visualization of earthquake phenomena. *Computers and Mathematics with Applications*, **66**(5), 647–658. <https://doi.org/10.1016/j.camwa.2013.02.003>
- [5]. Momani, S., & Odibat, Z. (2006). Analytical approach to linear fractional partial differential equations arising in fluid mechanics. *Physics Letters, Section A: General. Atomic and Solid State Physics*, **355**(4–5), 271–279. <https://doi.org/10.1016/j.physleta.2006.02.048>
- [6]. Ray, S. S., & Bera, R. K. (2005). Analytical solution of the Bagley Torvik equation by Adomian decomposition method. *Applied Mathematics and Computation*, **168**(1), 398–410. <https://doi.org/10.1016/j.amc.2004.09.006>
- [7]. Ghorbani, A., & Alavi, A. (2008). Application of He's variational iteration method to solve semi differential equations of nth order. *Mathematical Problems in Engineering*, **2008**, 1–9. <https://doi.org/10.1155/2008/627983>
- [8]. Fadravi, H. H., Nik, H. Saber., & R. Buzhabadi. (2011). Homotopy Analysis Method Based on Optimal Value of the Convergence Control Parameter for Solving Semi-Differential Equations. *Journal of Mathematical Extension*, **5**(2), 105–121.
- [9]. Çenesiz, Y., Keskin, Y., & Kurnaz, A. (2010). The solution of the Bagley-Torvik equation with the generalized Taylor collocation method. *Journal of the*

Franklin Institute, **347**(2), 452–466.  
<https://doi.org/10.1016/j.jfranklin.2009.10.007>

[10]. Saha Ray, S. (2012). On Haar wavelet operational matrix of general order and its application to the numerical solution of fractional Bagley Torvik equation. *Applied Mathematics and Computation*, **218**(9), 5239–5248. <https://doi.org/10.1016/j.amc.2011.11.007>

[11]. Mekkaoui, T., & Hammouch, Z. (2012). Approximate analytical solutions to the Bagley-Torvik equation by the fractional iteration method. *Annals of the University of Craiova, Mathematics and Computer Science Series*, **39**(2), 251–256.

[12]. Yuzbasi, S. (2013). Numerical solution of the Bagley-Torvik equation by the Bessel collocation method. *Mathematical Methods in the Applied Sciences*, **36**(3), 300–312. <https://doi.org/10.1002/mma.2588>

[13]. Mohammadi, F. (2014). Numerical solution of Bagley-Torvik equation using Chebyshev wavelet operational matrix of fractional derivative MSC: *International Journal of Advances in Applied Mathematics and Mechanics*, **2**(1), 83–91.

[14]. Krishnasamy, V.S., & Razzaghi, M. (2016). The Numerical Solution of the Bagley–Torvik Equation With Fractional Taylor Method. *Journal of Computational and Nonlinear Dynamics*, **11**(5), 051010. <https://doi.org/10.1115/1.4032390>

[15]. Mashayekhi, S., & Razzaghi, M. (2016). Numerical solution of the fractional Bagley-Torvik equation by using hybrid functions approximation. *Mathematical Methods in the Applied Sciences*, **39**(3), 353–365. <https://doi.org/10.1002/mma.3486>

[16]. Srivastava, H. M., Shah, F. A., & Abass, R. (2019). An Application of the Gegenbauer Wavelet Method for the Numerical Solution of the Fractional Bagley-Torvik Equation. *Russian Journal of Mathematical Physics*, **26**(1), 77–93. <https://doi.org/10.1134/S1061920819010096>.

[17]. Abu, Arqub, O., & Maayah, B. (2018). Solutions of Bagley–Torvik and Painlevé equations of fractional

order using iterative reproducing kernel algorithm with error estimates. *Neural Computing and Applications*, **29**(5), 1465–1479. <https://doi.org/10.1007/s00521-016-2484-4>

[18]. Jena, R. M., & Chakraverty, S. (2019). Analytical solution of Bagley-Torvik equations using Sumudu transformation method. *SN Applied Sciences*, **1**(3), 1–6. <https://doi.org/10.1007/s42452-019-0259-0>

[19]. Chui, C. K., & Lian, J. A. (1995). Construction of Compactly Supported Symmetric and Antisymmetric Orthonormal Wavelets with Scale 3. *Applied and Computational Harmonic Analysis*, **2**(1), 21–51

[20]. Mittal, R. C., & Pandit, S. (2018 b). Quasilinearized Scale-3 Haar wavelets-based algorithm for numerical simulation of fractional dynamical systems. *Engineering Computations*, **35**(5), 1907–1931. <https://doi.org/https://doi.org/10.1108/EC-09-2017-0347>.

[21]. Mittal, R. C., & Pandit, S. (2018). New Scale-3 Haar Wavelets Algorithm for Numerical Simulation of Second Order Ordinary Differential Equations. Proceedings of the National Academy of Sciences, India Section A: Physical Sciences, (ii). <https://doi.org/https://doi.org/10.1007/s40010-018-0538-y>

[22]. Mittal, R. C., & Pandit, S. (2017). Sensitivity analysis of shock wave Burgers' equation via a novel algorithm based on scale-3 Haar wavelets. *International Journal of Computer Mathematics*, (March), 1–25. <https://doi.org/10.1080/00207160.2017.1293820>

[23]. Das, S. (2011). Functional Fractional Calculus. In *Functional Fractional Calculus* (second). <https://doi.org/10.1007/978-3-642-20545-3>

[24]. Mittal, R. C., & Pandit, S. (2018c). Quasilinearized Scale-3 Haar wavelets-based algorithm for numerical simulation of fractional dynamical systems. *Engineering Computations (Swansea, Wales)*, **35**(5), 1907–1931. <https://doi.org/10.1108/EC-09-2017-0347>.

## Program for Example -1

```
clc; close all;format long
A=input('Enter the lower limit of support of Haar function -->');
B=input('Enter the Upper limit of support of Haar function -->');
J=input('Enter the Maximum level of resolution for Haar function -->');
M=3^J;M2=3*M;M3=3*M2;dX=(B-A)/(M2*1.0);
xbar=zeros(M2+1,1);x=zeros(M2,1);
h=zeros(M2,M2);R=zeros(M2,M2,M2);S=zeros(M2,M2,20);H=zeros(M2,M2);Z=zeros(1,M2);z=zeros(1,M2);
f=zeros(1,M2);Z1=zeros(1,M2);z1=zeros(1,M2);y1=zeros(1,M2); y=zeros(1,M2);G=zeros(M2,1);
%x(1)=0.1;
```

```

for l=2:M2+1
%x(l)=x(l-1)+0.1;
xbar(l)=A+(l-1)*dX;
if (l>1)
    x(l)=0.5*(xbar(l-1)+xbar(l));
end
end
for l=1:M2
    x(l)=x(l+1);
if((x(l)>=A)&&(x(l)<=B))
    f(l)=sqrt(pi)*((x(l)^(5/2))-(x(l)^(3/2))+2*(x(l)^(1/2)))+4*x(l)-1;
end
end
x(M2+1)=[];
for l=1:M2
fori=1:M2
    H(i,l)=sqrt(pi)*x(l)*(h(i,l)+R(i,l,5)+R(i,l,20))- (sqrt(pi)*(x(l)^(3/2)))+1)*S(i,1,20);
end
end
c=f/H;
for l=1:M2
    y(l)=0;
fori=1:M2
    y(l)=y(l)+(c(i)*(R(i,l,20)-x(l)*S(i,1,20)));
end
    y(l)=y(l)+x(l);
    y1(l)=x(l)^2;
end
figure(1)
plot(x,y,'-o')
hold on
plot(x,y1,'-r')
title(['Numerical Experiment No.1'],'FontSize',20)
xlabel(['t'],'FontSize',20)% x-axis label
ylabel(['x(t)'],'FontSize',20) % y-axis label

```

```

legend({'Exact Solution','Numericalsolution'},'Location','Southwest','FontSize',20)
hold off
figure(2)
sum=0;sum1=0;
for l=1:M2
    Z(l)=(abs(y(l)-y1(l)))^2;
    sum=sum+Z(l);
    sum1=sum1+(y1(l)^2);
    z(l)=abs(y(l)-y1(l));
end
L2=sqrt(sum)/sqrt(sum1)
Linf=max(z)
plot(x,z,'rp-')
hold on
title(['Numerical Experiment No.1'],'FontSize',20)
xlabel(['t'], 'FontSize',20);
ylabel(['y_{"Exact"}(t) -- y_{"Approximated"}(t)'], 'FontSize',20);
where h represents the Haar function, R integral of Haar function, S is the integral of Haar function at t=1.

```